AN INVESTIGATION OF CLINICAL FEASIBILITY; APPLYING SPATIALLY FRACTIONATED RADIOTHERAPY (GRID) TREATMENTS TO A HELICAL TOMOTHERAPY UNIT

By

MacKenzie R. Hill

A THESIS

Presented to the Department of Medical Physics
and the Oregon Health & Science University School of Medicine
in partial fulfillment of the requirements for the degree of

Master of Science

June 2018

School of Medicine

Oregon Health & Science University

CERTIFICATE OF APPROVAL

This is to certify that the Master's thesis of

MacKenzie R. Hill

Has been approved

Mentor/Advisor

Member

Member

TABLE OF CONTENTS

Abstract

Background: GRID therapy is an atypical heterogeneous method of delivering dose to a treatment volume that came about in the early 1900's, but disappeared with the invention of modern linear accelerators. The modern use of GRID therapy takes advantage of its unique ability to gain clinical results with deep-seated, bulky, or radioresistant tumors. Historically GRID therapy was completed with the use of a physical cut-out applicator attached to the head of a linear accelerator. However with advantages of modern technology we now have the ability to use inverse planning in the creation of virtual GRID patterns. Recent research suggests the Helical TomoTherapy treatment unit as favorable approach to delivering virtual GRID treatments. The biologic studies of GRID therapy strongly suggest the increased response from GRID therapy due re-oxygenation of hypoxic tumor volume and bystander effects.

Methods: The clinical feasibility of GRID therapy applied to the Helical TomoTherapy unit was done in a way to align with the OHSU present workflow and software. The TomoTherapy "cheese" phantom was simulated with our Phillips Big Bore CT simulator. The test regions to be irradiated within the phantom were contoured with the Eclipse treatment planning system. Irradiation delivery QA analysis was completed with the PTW Octavius 729 ion chamber, as well as film dosimetry. The 2D cores and 3D sphere GRID treatment volumes studied simulate those that previous studies indicated as successful. The planned tumor GTV was a rough 13 cm diameter sphere. The studied cores had a diameter of 15 mm and were spaced about 5 cm center to center. The spheres studied had a 15 mm diameter and were placed with a 5-6 cm distance center-to-center.

All 3 studied treatment volumes were developed on the Helical TomoTherapy TPS to an optimal dose distribution.

Results: The planed times for all fields were longer than 40 minutes and fractionated to achieve deliverable plan times. Plan quality assurance completed with the PTW Octavius 729 phantom and ion chamber array indicated that the measured coronal dose plan matched the computed plane with an absolute gamma value of 95% or better with parameters of distance-to-agreement of 2.0 mm and a dose difference with reference to the maximum dose of calculated volume of 2.0%. Visual inspection of the processed and scaled film indicated an acceptable agreement of planned and measured sagittal dose plane with minimal normalization.

Conclusions: The results from this study indicate that it is possible to deliver high dose spatially fractionated plans with a Helical TomoTherapy unit with either 2D cores or 3D spheres. The data shows that with the current plan settings of pitch 0.287 and a fixed jaw setting of 1.05 cm plans created have total delivery times that are greater than 40 minutes. These plans are too long for both the machine and patients to complete in one pass, the total plan needs to be fractionated to achieve deliverable times. The analysis of 2D and 3D GRID plan values indicates that the 3D GRID sphere geometry has the best qualities for treating real patients. The 3D GRID plan has the lowest treatment time, achieves planned dose maximums within the treatment cores, yet also has the lowest average phantom dose. The quality assurance results show that the machine is completely capable of delivering the heterogeneous fields, but there is a complication requiring more scheduled time in order to reasonably achieve this in a clinical setting. This preliminary

study indicates that with further investigation, the 3D GRID spheres show great promise for clinical implementation.

1. Introduction

1.1. GRID Therapy

GRID therapy or Spatially Fractionated Radiotherapy, is a unique method of radiation therapy that distributes a heterogeneous peak and valley pattern of dose (15-20 Gy) in a single fraction to a tumor or treatment volume [1]. This is atypical because the current methodology within the field of radiation oncology is to a deliver a highly homogenous dose to the treatment site, while also maintaining a rapid dose reduction outside of the treatment volume.

The original purpose for this heterogeneous dose distribution was an attempt to spare the skin of radiation therapy patients in the early 1900's [2]. At this time the field of radiation therapy was dominated by treatment devices that utilized either low energy x-ray machines or radioactive isotopes for treatment. Due to the relatively low energies and a short treatment distance, these particles deposited a majority of their energy at 0.5 cm or less from the surface of the skin [3]. The dermis, epidermis and subcutaneous layers of the skin are about 0.8 cm deep [4]. This means the low photon energies used deposit a majority of their dose in the skin. This energy deposition causes cellular damage of the skin, and manifests as erythema or ulceration.

Therefore, in order to reduce the surface area of the skin receiving high doses of radiation while still achieving high doses of radiation to a more internal treatment location, the method of GRID therapy was adopted. This allowed for areas of healthy tissue to be interspersed with irradiated tissue and allow for improved wound healing.

1.1.2 GRID History

Originally, forms of GRID therapy were made using leaded rubber; however there are several adaptions that grew over time. Current adaptions include using Cerrobend or brass, with holes cut in them that can be attached to treatment heads of machines."

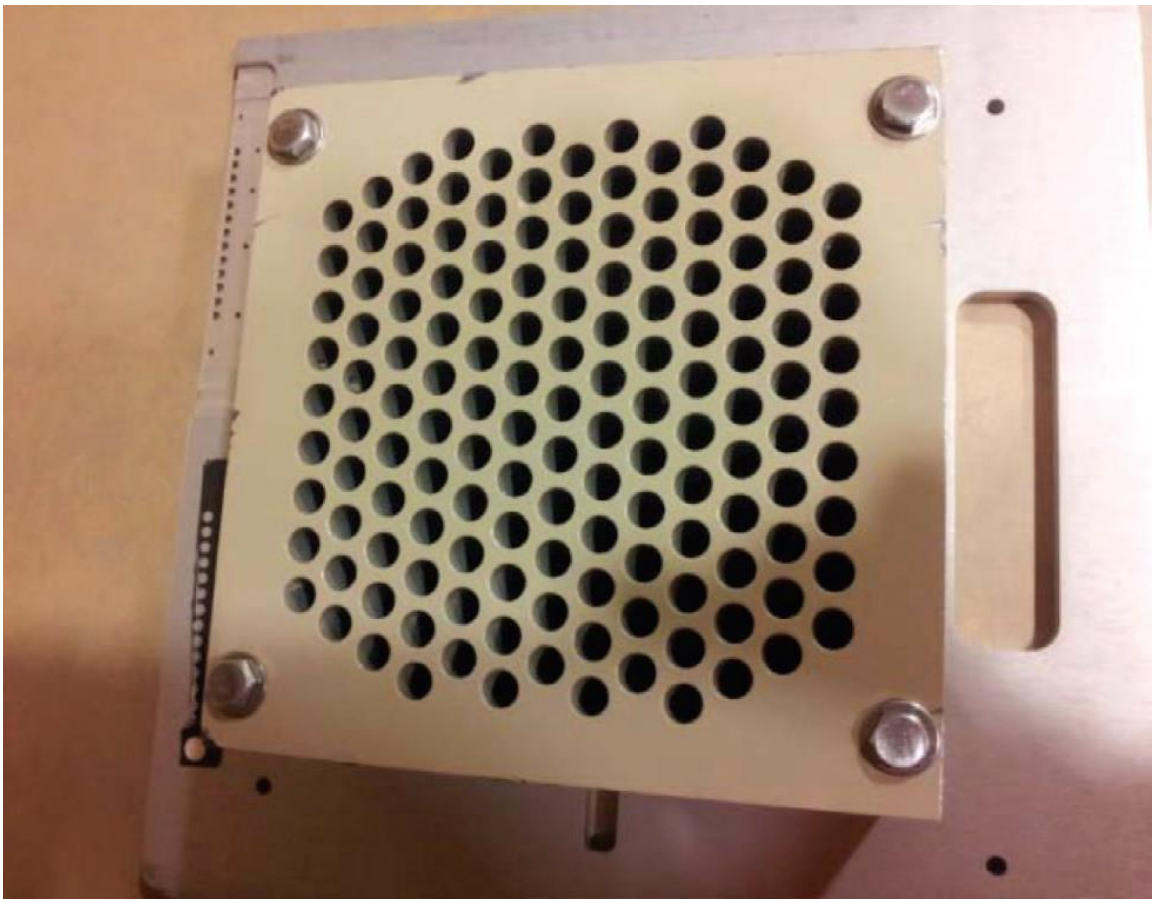

Figure 1. GRID Compensator by Zhang, X., Penagaricano, J., Yan, Y., Sharma, S., Griffin, R. J., Hardee, M., … Ratanatharathom, V. (2016). Application of Spatially Fractionated Radiation (GRID) to Helical Tomotherapy using a Novel TOMOGRID Template. *Technology in Cancer Research & Treatment*, *15*(1), 91–100. https://doi.org/10.7785/tcrtexpress.2013.600261, copyright under Creative Commons Attribution-NonCommercial 3.0 License [7]

As the treatment systems used for radiation oncology progressed the use of Intensity Modulated Radiation Therapy (IMRT), Volumetric Arc Therapy (VMAT), and higher energy beams became commonplace. The need for skin sparing capabilities provided by GRID therapy diminished, and GRID therapy nearly disappeared. Yet some investigators observed that there was something unique about the response difficult tumors exhibited after GRID therapy. Inspection into the properties of this response needed to be investigated.

It was discovered that GRID therapy could be extremely effective at treating deep seated and bulky (larger than 8 cm) tumors, as well as tumors that were typically radioresistant, or grew during treatment. Presently the community of radiation oncology is shifting toward 2D GRID patterns created through MLC modulation and 2D or 3D virtual GRIDs created with the help of inverse planning systems. Nonetheless physical GRID therapy applicators are still commercially available, and have applications in treating large-external-spherical tumors.

1.1.3 Virtual GRID Research

With the recent resurgence of GRID therapy, clinics have been investigating different methods for delivering heterogeneous dose patterns to the treatment volume. Researchers in the Department of Radiation Oncology, School of Medicine, University of Arkansas for Medical Sciences (UAMS) have been investigating virtual core GRID patterns for Helical Tomotherapy (HT-GRID) [1], [6], [7]. The methodology at UAMS started by trying to match virtual GRID to the dose distribution of commercially available

physical GRID applicators; these GRID applicators already had a history of positive clinical results.

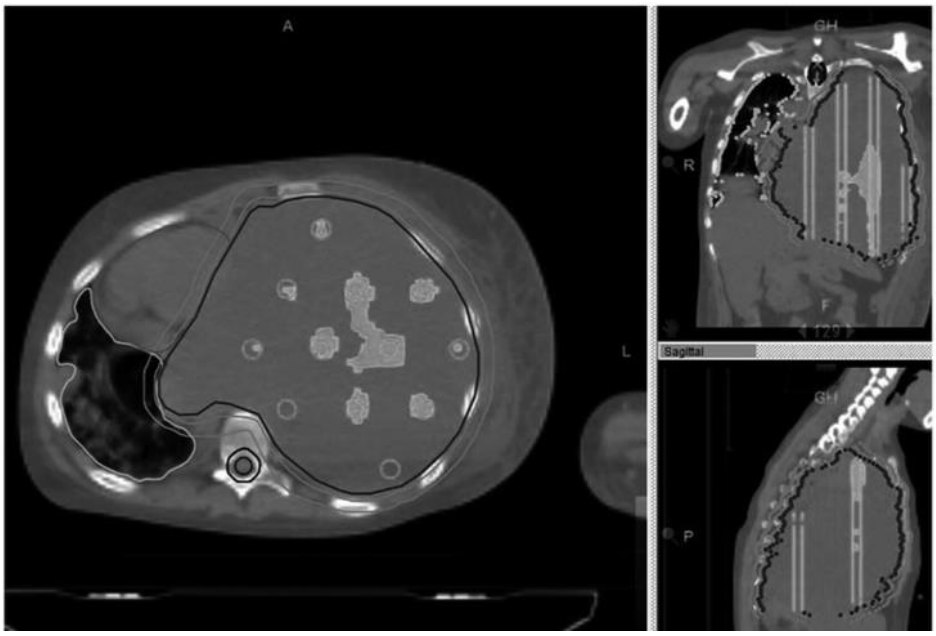

Figure 2. Core HT-GRID by Narayanasamy, G., Zhang, X., Meigooni, A., Paudel, N., Morrill, S., Maraboyina, S., … Penagaricano, J. (2017). Therapeutic benefits in grid irradiation on Tomotherapy for bulky, radiation-resistant tumors. *Acta Oncologica*, *56*(8), 1043–1047. https://doi.org/10.1080/0284186X.2017.1299219, copyright under CC BY-NC-ND [1]

This Arkansas group has investigated many components of HT-GRID including comparisons with physical GRID gross tumor volume (GTV) distributions, doses to organs at risk (OAR), target dose inhomogeneity, and therapeutic advantages. One of the clinical applications created by UAMS is their own DICOM editor called DICOMan. This editor allows the convenience of quickly and efficiently creating a variety of GRID arrangements within a contoured GTV. It gives the user the ability to control shape, pattern type, and geometry. When testing the geometric dose distributions of a virtual HT-GRID, machine capabilities and particle physics play a large role.

The two 2D GRID core structures studied at UAMS included treatment volumes with the diameters of 13 mm and 16 mm paired respectively with center-to-center distances of 54 mm and 45 mm [6]. In creating treatment plans for these cores a 1 cm field width, 0.215 pitch, and a 2.5 modulation value were applied. The test showed that the core pattern with the 16 mm openings pared with a 45 mm center-to-center geometry provided the best peak to valley ratio and the this dose distribution, and was more comparable to that observed with a physical grid [6].

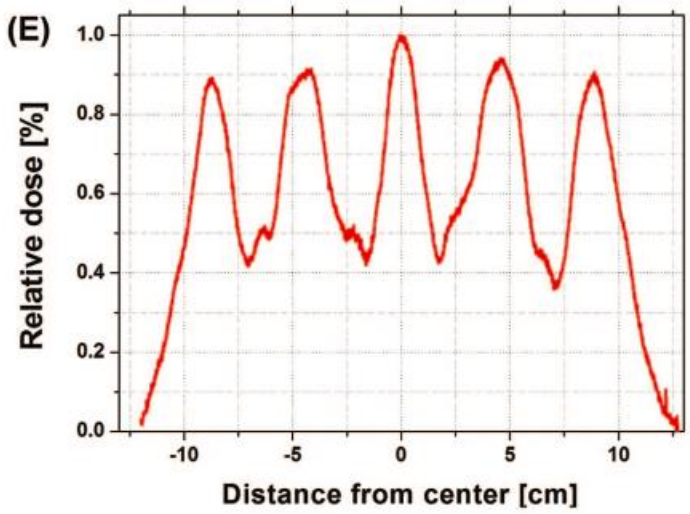

Figure 3. Core With 16 mm Diameter and Center-To-Center of 45 mm by Zhang, X., Penagaricano, J., Yan, Y., Sharma, S., Griffin, R. J., Hardee, M., … Ratanatharathom, V. (2016). Application of Spatially Fractionated Radiation (GRID) to Helical Tomotherapy using a Novel TOMOGRID Template. *Technology in Cancer Research & Treatment*, *15*(1), 91–100. https://doi.org/10.7785/tcrtexpress.2013.600261 , copyright under Creative Commons Attribution-NonCommercial 3.0 Lice **[6]**

In physical GRID application treatments there is very little control of the location of the maximum dose, resulting in the maximum dose falling outside of the tumor volume. Alternatively, HT-GRID treatments distributed the maximum dose within the treatment volume [1]. These studies have shown that HT-GRID has the ability reduce

maximum dose to normal tissue and OAR doses, while also increasing the valley peak ratio of doses within the targeted tissue.

In investigating the linear quadratic mod el of large-bulky-radioresistant tumors, the therapeutic ratio for a single fraction of GRID therapy was determined to be 15-20 Gy. This therapeutic advantage for GRID therapy was determined by comparing the results of conventional treatments (2 Gy per fraction) and GRID therapy treatments [1]. Figure 4 illustrates that as tumors become more radioresistant, or have increased tumor survival fractions, that the therapeutic advantage of GRID therapy becomes more prominent. This agrees with the clinical results of Mohiudin et al, later discussed in this paper.

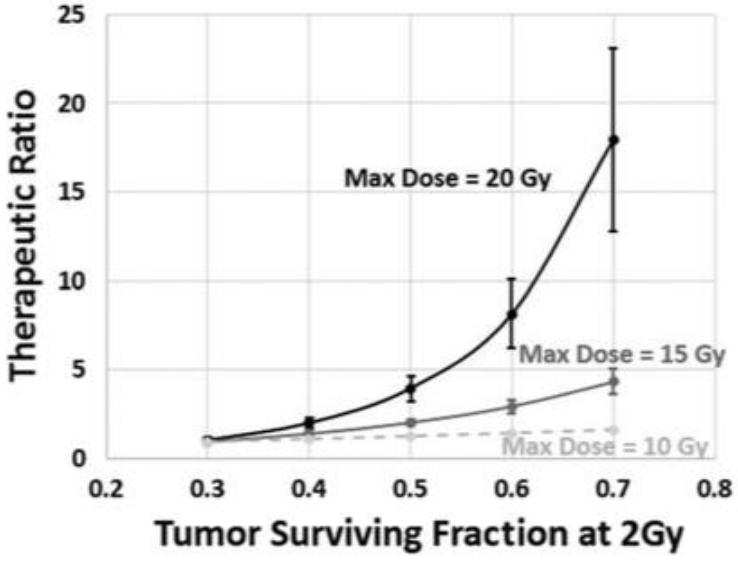

Figure 4. GRID Therapeutic Ratio by Narayanasamy, G., Zhang, X., Meigooni, A., Paudel, N., Morrill, S., Maraboyina, S., … Penagaricano, J. (2017). Therapeutic benefits in grid irradiation on Tomotherapy for bulky, radiation-resistant tumors. *Acta Oncologica*, *56*(8), 1043–1047. https://doi.org/10.1080/0284186X.2017.1299219, copyright under CC BY-NC-ND [1]

The test of clinical applications at UAMS showed that the virtual HT-Grid was able to treat patients as effectively as the physical GRID applicator, if not better when the tumor size or location became complex. While the physical grid was easier to complete in the planning stage, the virtual HT-Grid was more effective at sparing normal tissue and OARs. In one scenario there was a reduction to the spinal cord dose from 1577 cGy with the GRID applicator to 355 cGy with the HT-GRID [7].

Recent investigations of lattice therapy, a more modern example of GRID therapy, in the form of 3D spheres has shown promise. In 2009, Wu et. al described this process and discussed the flawed method of matching 2D grid pattern to the historical applicators when our modern capabilities allow us to plan and irradiate 3D structures [8].

At the Innovative Cancer Institute in Miami, Florida Beatriz E. Amendola's group have published a collection of articles citing their success of treating patients with lattice therapy or 3D GRID therapy. These papers compare this heterogeneous dose deposition from GRID therapy to that of interstitial brachytherapy [9]. The published cases state a history of using this methodology, but specifically recorded 2 case studies, a large metastatic mixed Mullerian ovarian tumor and a locally advanced lung tumor[9], [10]. Both tumors reported were historically difficult to treat[9], [10].

The Mullerian ovarian tumor patient was treated concurrently with conventional fractionation radiotherapy, and later paired with both chemotherapy and surgical removal, and 6 weeks post lattice therapy showed a complete pathological and clinical response [9]. More recently a patient was treated with locally advanced squamous cell carcinoma of the lung. After having poor results with chemotherapy, a 3D GRID or lattice therapy plan was created. The spheres used in the 3D grid plan where 1.5 cm in diameter and

spaced out to create a GRID pattern. The patient received a combination of both 3D GRID therapy as well as a conventionally fractionated plan. After 6 years the patient has no evidence of disease (NED), and only has minor damage post irradiation [10]. These cases, though anecdotal, show promise for the future and record clinical outcomes post treatment for both patients. These plans were created through VMAT inverse planning methods and use of a linear accelerator.

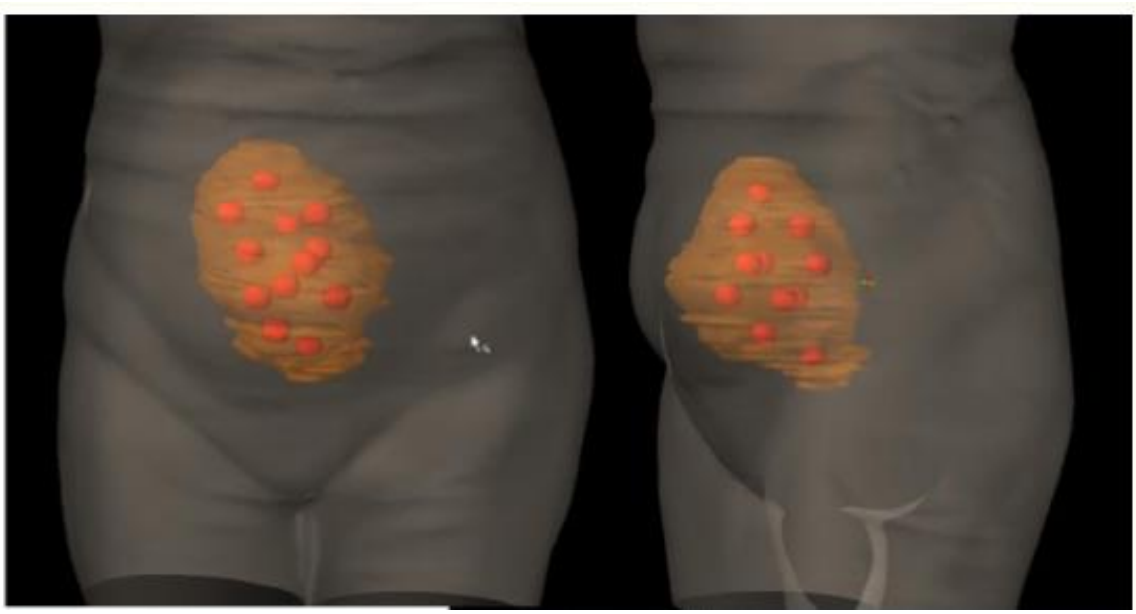

Figure 5. Sphere GRID by Blanco Suarez, J. M., Amendola, B. E., Perez, N., Amendola, M., & Wu, X. (n.d.). The Use of Lattice Radiation Therapy (LRT) in the Treatment of Bulky Tumors: A Case Report of a Large Metastatic Mixed Mullerian Ovarian Tumor. Cureus, 7(11). https://doi.org/10.7759/cureus.389, copyright under Creative Commons Attribution License CC-BY 3.0 **[9]**

1.1.4 GRID Clinical Results

The major clinical evidence in favor of GRID therapy's efficacy comes from the publications of Mohiuddin et al. His work shows extensive clinical success with GRID

therapy in treating Sarcomas, Melanomas, head and neck tumors, and colorectal cases [11]. Though these results were achieved by treating with a physical GRID applicator, the results may be easily translated to some modern virtual GRIDs. Plans such as 2D GRIDs, which have analogous dose distributions to the original physical GRID applicators, may achieve the most similar responses. Mohiuddin's data supports the efficacy of GRID therapy and its need for growth and revival within the field of radiation oncology.

TABLE 2. Clinical total response of grid therapy for tumors with different histological characteristics and treatment sites. The numbers in the parentheses for each tumor type represent the total response under grid therapy.

References	*Tumor Histology or Site*				
Mohiuddin et al.[18]	Osteosarcoma (100%)	Liposarcoma (50%)	Leiomyosarca (100%)	Colorectal (100%)	
Mohiuddin et al.[19]	Sarcoma (94%)	SCC (92%)	Melanoma (83%)	Adenocarcinoma (69%)	
Mohiuddin et al.[9]	Sarcoma (83%)	SCC (94%)	Adenocarcinoma (94%)	Melanoma (50%)	
Sathishkumar et al.[10]	SCC (100%)	Adenocarcinoma (More that 90%)	Melanoma (More than 80%)		
Huhn et al.[7]	SCC of H&N (93%)				
Peñagaricano et al.[20]	Parotid (0%)	Base of tongue (30%)	Maxillary sinus (50%)	Nasopharynx, Retromolar trigone, and Larynx (100%)	Tonsil (25%)

Figure 6. Table 2. By Gholami, S., Nedaie, H. A., Longo, F., Ay, M. R., Wright, S., & Meigooni, A. S. (2016). Is grid therapy useful for all tumors and every grid block design? *Journal of Applied Clinical Medical Physics*, *17*(2), 206–219. https://doi.org/10.1120/jacmp.v17i2.6015, copyright under Creative Commons Attribution License **[11]**

A Case study reported by Mohiuddin et al. recorded a patient with a locally advanced Melanoma who benefited from GRID therapy. A 53 year old male presented with a large mass on the left of his neck, the original treatment involved starting on a high dose interleukin-2 (IL-2) and showed no response [12]. The patient was then given monoclonal antibodies and chemotherapeutic drugs, but the tumor was still progressing.

After about 7 months of systemic attempts to treat the tumor a radiation therapy plan was set in place for co-planar physical applicator GRID therapy paired with a conventional fractionation scheme, while concurrent chemotherapy was maintained. 5 months later the patient had complete resolution of the large mass with no adverse side effects, and 12 months post irradiation showed no sign of recurrence [12].

Figure 7. Patient Neck Tumor Results from GRID Therapy by Mohiuddin, M., Park, H., Hallmeyer, S., & Richards, J. (n.d.). High-Dose Radiation as a Dramatic, Immunological Primer in Locally Advanced Melanoma. *Cureus*, *7*(12). https://doi.org/10.7759/cureus.417, copyright under Creative Commons Attribution License CC-BY 3.0 **[12]**

1.2 Radiation Biology

In the 1930's the advantage of GRID therapy related to its skin sparing capabilities. However, now that modern devices for radiation therapy have abilities that

allow them to achieve the same or better levels of skin sparing, it is pertinent to describe the current clinical relevance of GRID therapy. Mohiuddin and other researches have shown the unique benefits GRID therapy in treating radioresistant, tumors [11].

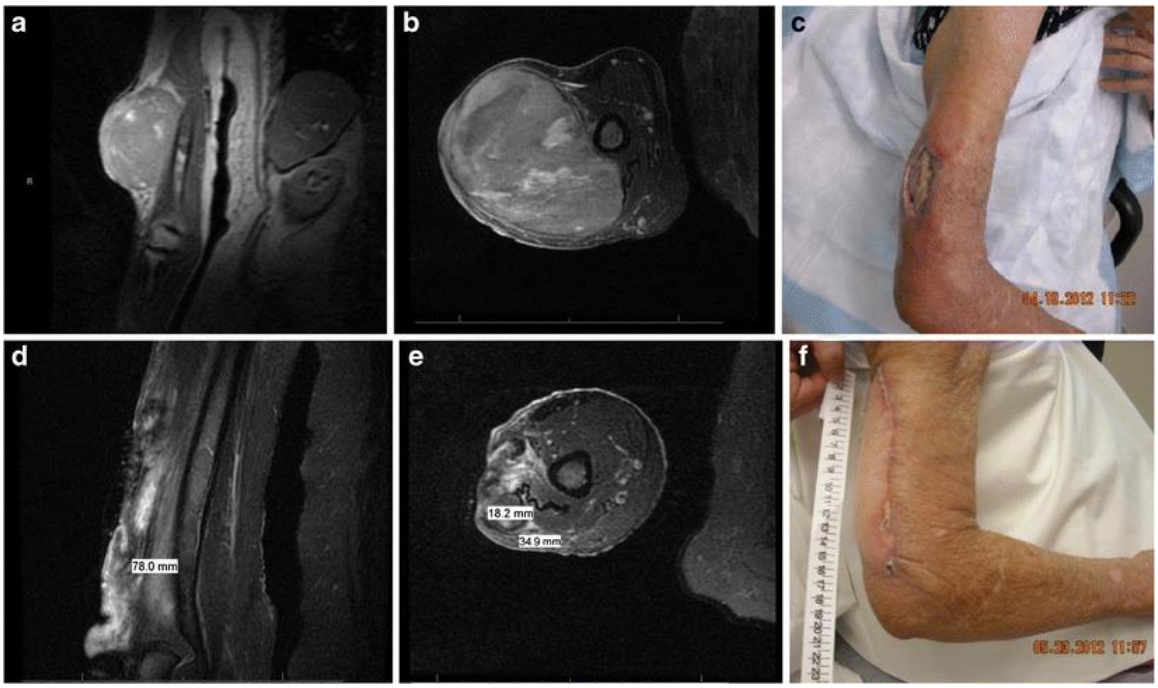

Figure 8. Clinical response to GRID therapy by Kaiser, A., Mohiuddin, M. M., & Jackson, G. L. (2013). Dramatic response from neoadjuvant, spatially fractionated GRID radiotherapy (SFGRT) for large, high-grade extremity sarcoma. *Journal of Radiation Oncology*, *2*(1), 103–106. https://doi.org/10.1007/s13566-012-0064-5, copyright by Creative Commons Attribution License CC-BY 3.0. **[13]**

It was not long after the discovery of radiation in the late 1800's that people started noticing the detrimental effects on the body. Roentgen's wife died of leukemia, Marie Curie died of aplastic anemia, and the watch painters named the "Radium Girls" had jaw cancer [14]. Yet scientists also realized the benefit of radiation for damaging unwanted cells or cancer. As early as 1910 with the use of higher energy x-ray tubes the treatment of skin cancer was possible [15]. Radiobiology grew out of the need to understand the responses achieved.

In Eric Hall's Radiobiology for the Radiologist, the concepts of the DNA damage, therapeutic ratio, linear energy transfer (LET), cell cycling, DNA repair mechanisms, the bystander effect, oxygenation, circulation, and cell signaling are discussed. It is the current understanding that these are some of the mechanisms that increase the effectiveness of GRID therapy [16]. Later these advantages will be discussed in their relationship to GRID therapy.

The primary method of cell killing and damage done by radiation is based on the ability of ionizing radiation to damage DNA. This DNA damage can create irreparable base pair connections within the nucleus of the cell. There are two main methods in which DNA is damaged by ionizing radiation, direct and indirect damage. Direct damage occurs when the radiation interacts directly with the DNA strand. Indirect damage occurs when the radiation first interacts with the water in the nucleus of the cell creating a free radical. That free radical can then go forward and damage DNA. Indirect damage is more common in low linear energy transfer (LET) forms of radiation like photons or x-rays.

Oxygen plays a role in the ability of a cell to repair DNA damage. When DNA damage occurs Oxygen has the ability to react with the DNA strand at the location of the damage preventing the repair, one of the many cellular responses to DNA damage. While this occurrence in healthy tissue is an unfortunate reality, it plays a large role in the effectiveness of radiation therapy in tumor cells. The oxygen enhancement ratio or OER is a concept that proves the importance of oxygen concentration in cell kill for low LET radiation.

Unfortunately as tumors grow, the vasculature supporting the structure often becomes erratic and leads to poor internal circulation. Poor circulation means low oxygen levels or a state of hypoxia, this hypoxia gives tumor cells a resistance against radiation therapy. This is why reoxygenation and repair of the hypoxic tumor is important to achieving a clinical response in radiation therapy. This reoxygenation and repair are what allow further treatments to become effective.

The therapeutic ratio is the ratio of cancer cells killed in comparison to normal tissue cells. This is scientifically studied by using the concept of surviving fractions (SF), or the count of healthy cells in normal tissue after receiving radiation, in comparison to the originally plated cell count. The main methodology behind fractionated radiation therapy is to maximize this therapeutic ratio. In order to model the cell damage created by radiation, current studies utilize the linear quadratic theory. The linear quadratic model is a method utilizing statistically derived parameter to describe cell death and survival after being irradiated. If an extremely high dose can be given to the tumor cells, while the normal tissue cells receive a much lower dose, an extreme difference in cell kill can be achieved. This is why GRID therapy aims to deliver roughly 15-20 Gy to portions of the tumor volume, and only 1-2 Gy to the normal tissue.

The relative biologic effectiveness (RBE) for each cell line is part of what creates these disparities leading to the therapeutic ratio. The main factors controlling the RBE of radiation are LET, radiation dose, dose per fraction, dose rate, and biologic end point. Increasing the dose to cells is a quick and easy method to achieve a higher cell death rate overall, but this higher cell death rate affects both the cancer cells and healthy tissue cells. At some point the damage to healthy tissue drastically disrupts the regular function

of that organ or tissue. This concept applies to all areas of RBE, the goal is to maximize the efficiency of the process, and gain the largest ratio or advantage possible.

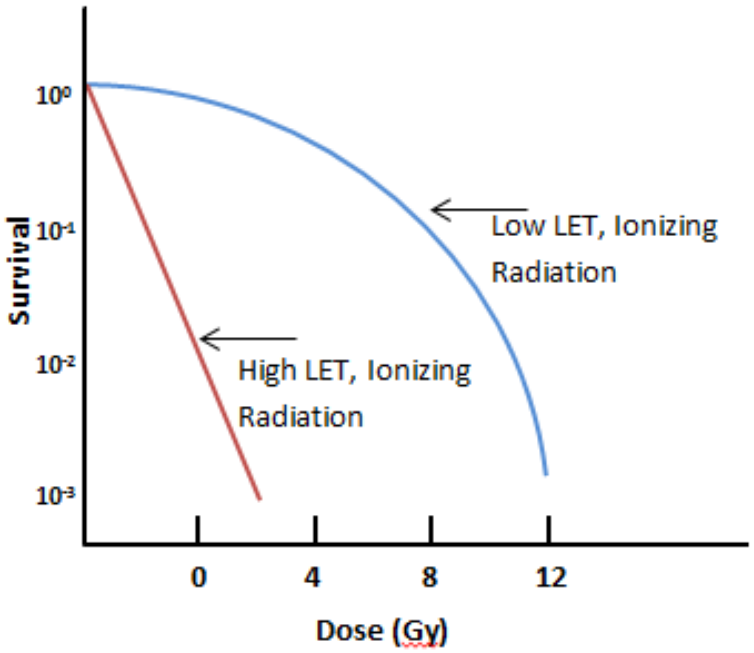

Figure 9. Linear Quadratic Model Example

The bystander effect is a unique process in which unirradiated cells in contact with irradiated cells undergo apoptosis or cell death even though they have not been irradiated themselves. The bystander effect was has been studied by Asur et al. wherein it showed that the cell kill achieved was not due to scatter or low dose regions, but in fact a complex collection of cell signaling mechanisms that do not only rely on the cellular gap junction [17]. In animal cells gap junctions are a specialized form of cellular connections or pores that allows a direct pathway for molecules between the cytoplasm of the two cells involved.

1.2.2 Bystander Effect

The Mechanisms of Radiation-Induced Bystander Effect by Najafi, Fardid, and Hadadi published in 2014 is a modern in depth discussion of the mechanisms behind the observed bystander effect [18]. This paper breaks down the process in to 5 mechanisms: immune system, free radicals, oxidative stress, changes of gene expression of inflammatory pathway, and epigenetic modulators [18]. The immune system is a biologic pathway in the body with the intent to protect us from inflammation and disease. The molecules used to create a systemic immune response are called cytokines.

Cytokines are important to consider in response to radiation because they have the ability affect cell proliferation. Specifically in response to radiation, cells can stimulate production of IL-1, IL-2, IL-6, IL-8, TNFα and TGFβ even when they have not been directly irradiated. The cellular response to the production of these cytokines is twofold. Tumor Necrosis Factor alpha (TNFα) has the unique ability upregulate tumor cell death, while normal tissue remains maintains a stable rate of cellular damage. Conversely many of these other cytokines, like interleukins, have been shown to increase DNA damage systemically [18]. While the concern of secondary malignancy from these adverse bystander effects may arise, it is important to recall that GRID therapy is often used palliatively or in worse case scenarios for advanced cases, and the time needed for development of these secondary malignancies, 20 years, is not realistic.

Oxidative stress occurs in the presence of free radicals. Free radicals can form in the body when radiation collides with water. Free radicals typically have a short life span due to their chemical instability, and therefore have a limited physical range of damage within the body. However, the presence of oxygen free radicals can produce long-lived

peroxides. With an increased lifespan these peroxides can travel farther in the body. This increased lifespan has been shown to play a role in the damage of non-irradiated cells [18]. These peroxides may decrease the need for local oxygen concentrations, and aid in the cell death of hypoxic tumor cells.

1.2.3 GRID Bystander Effect

In studying patient outcomes from GRID therapy and tracking the corresponding cellular responses, research groups have been able to find correlations with the bystander effects and clinical efficacy of GRID therapy. A study at the University of Kentucky investigated the systemic responses of patients receiving GRID therapy. This systemic responses tracked were the cytokines TNFα and TGFβ detectable in the bloods serum [19]. TNFα or Tumor Necrosis Factor alpha, is a cytokine that has been shown to upregulate tumor cell death when present [19]. TGFβ or Transforming Growth Factor beta, has been shown to inhibit primary tumor development, but as tumors progress they become resistant to the growth inhibitory properties of TGFβ[20]. In a large portion of the population studied, 21 out of 31, no TNFα levels were detectable. However in the population where TNFα was detectable, there was a strong correlation between clinical response and TNFα. The TGFβ serum concentrations were more easily detected in the patient samples, but showed no correlation with clinical response [19].

The University of Arkansas for Medical Sciences did a study on the bystander effects of GRID therapy using single high dose brass grid collimated beams to irradiate Murine SCK mammary carcinoma cells and SCCVII squamous carcinoma cells [21]. In this study they examined an extensive list of DNA genes controlling DNA repair,

apoptosis, cellular response to stress and cell cycling in both directly irradiated and non-irradiated or bystander cells. These cells were studied at 0 hours,4 hours, and 24 hours after irradiation, and were compared with controls.

Some of their conclusion include that GRID therapy leads to an increased systemic cytokine production, a large increase in expression of antioxidants genes in response to oxidative stress (free radicals), and an increase in expression of DNA repair genes [21]. While this study was not tested *in vivo*, it directly agrees with the mechanisms set out by the Najafi et al. paper, and increases strength for the argument that the bystander effect is one reason GRID therapy is so potent.

1.3 Helical Tomotherapy

Accuray's TomoTherapy is a unique approach to the modern accelerator therapy. A Helical TomoTherapy unit takes the helical approach of modern computed tomography (CT) scanners, and combines it with the principles of a linear accelerator, creating tomo or slice therapy. Similar to a CT scanner, Helical TomoTherapy units have an inner spinning doughnut mechanism with attached electronics. The treatment units attached to this mechanism include a compact linear accelerator capable of a 6 MV Flattening Filter Free (FFF) beam, an MV detector array, Jaws capable of 5.0 cm, 2.5 cm, and 1 cm axial widths, and Binary MLCs. Comparable to a modern CT scanner, the treatment head rotates about the machine while the patient is fed through the center of the machine with a mechanical table [22].

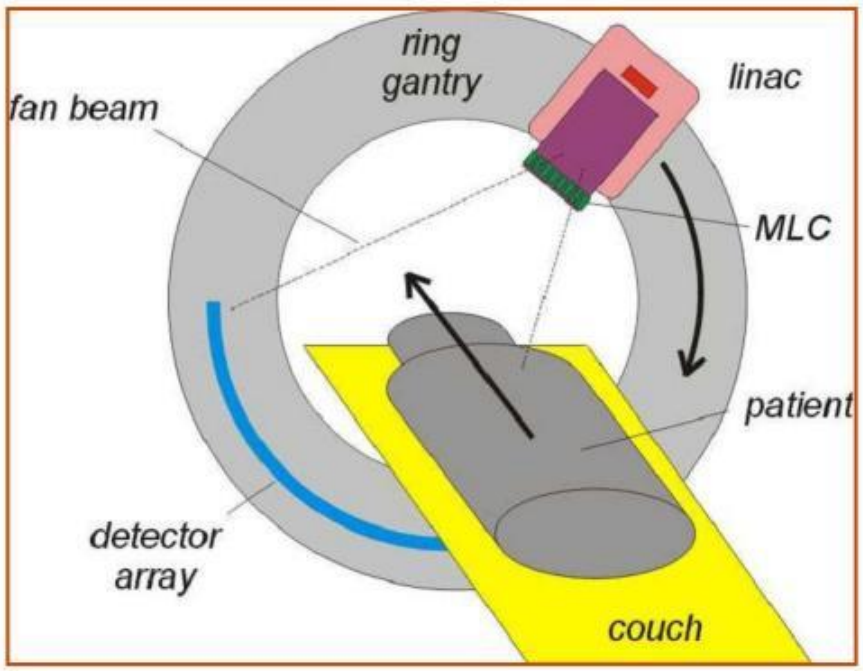

Figure 10. TomoTherapy Diagram by Schematic drawing of a helical tomotherapy unit. (n.d.). Retrieved May 31, 2018, from https://www.researchgate.net/figure/Schematic-drawing-of-a-helical-tomotherapy-unit_fig2_51166856, copyright under CC BY-SA **[23]**

Due to its similarities to CT scanners the TomoTherapy treatment unit also has pitch considerations. Pitch is a value that describes how much the beam overlaps or is spaced out as it rotates. A pitch less than 1 indicates overlap of the beam edges as it rotates around the field, while a pitch greater than 1 indicates a gap between the edges of the beam as it rotates around the field.

Pitch = (Table Travel Distance / Beam Width)

Due to the effects of beam divergence and penumbra, there are optimal pitches that minimize the inherent threading effect in the delivery of dose fields. This threading effect manifests itself as a ripple of the dose distribution within treatment zones [24]. In order to avoid this dose ripple there are recommended paired pitch and jaw settings. A pitch setting of 0.287 is among these optimum pitches.

The TomoTherapy unit has the ability to treat field as long as 160 cm, as well as a competency with treating more typical cases like breasts or prostates. The workflow for Helical TomoTherapy typically includes an MVCT of every patient before treatment. The TomoTherapy unit has a binary MLC system which gives it the modulation needed to treat complex cases such as head and neck tumors. These machine parameters allow for increased field sizes as well as a ready ability to conform to targets and avoid OAR. This makes the TomoTherapy unit a good candidate for virtual GRID therapy.

2. Materials and Methods

In investigating the clinical feasibility of implementing a GRID therapy protocol, it is pertinent to consider many of the steps in the process and attempt to match some of the clinical processes in use. To begin, the treatment simulation was done using a TomoTherapy QA cheese phantom and scanned with an onsite Philips Big Bore Brilliance CT sim scanner. To simulate patient heterogeneities a variety of density, cores were placed in the scanned phantom.

Figure 11. TomoTherapy "Cheese" Phantom

The scan data was then loaded to the Varian Eclipse treatment planning system (TPS) where all contours were completed per our clinics protocol. In order to test the range clinical capabilities a large simulation tumor, a 1270 cc sphere roughly 13 cm in diameter was contoured as the GTV.

Two core GRID distributions were analyzed to test the full spectrum of capabilities of the machine, one parallel (anterior/superior) and one perpendicular (inferior/superior) to the direction of beam. The creation of the virtual 2D GRID 15 mm diameter rods with 50 mm center to center geometry were contoured along the anterior/posterior plane as well as in the inferior/superior plane. The anterior/posterior cores had a volume of 70 cc, while the inferior/superior cores had a volume of 90 cc. The 3D virtual GRID spheres were created with a 15 mm diameter, spaced with at least a 50

mm center to center geometry, and contained roughly 12 cc. All GRID patterns tested in this experiment were mocked to match reported geometries in previously successful studies. Post-planning analysis software was utilized to derive proper dose values for volume averages and maximums.

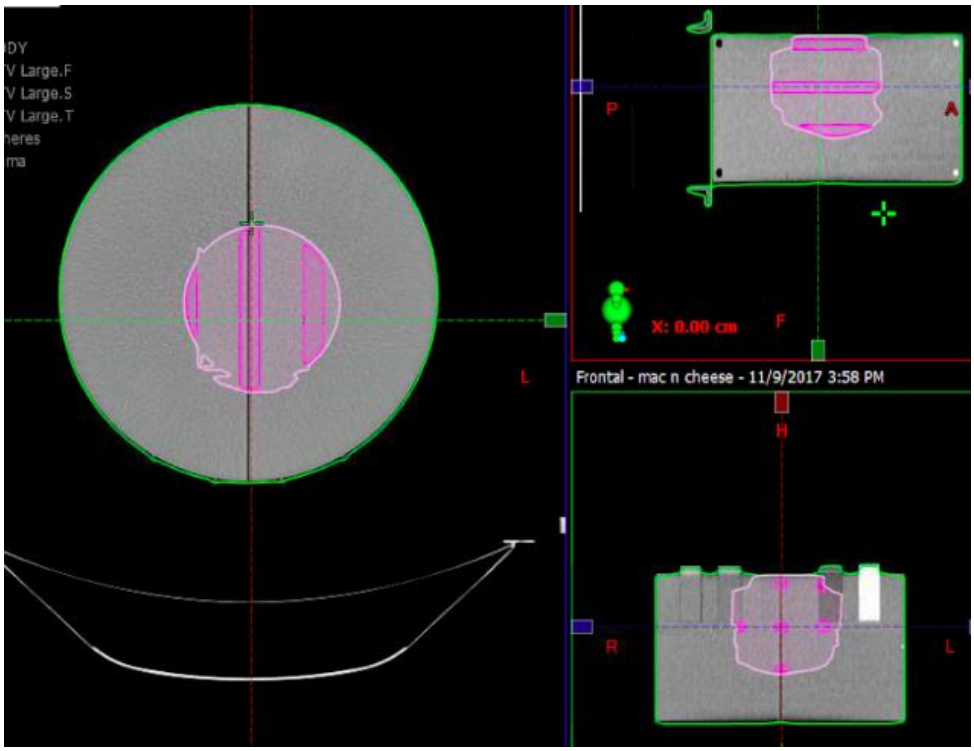

Figure 12. Anterior Posterior GRID cores created with Eclipse TPS

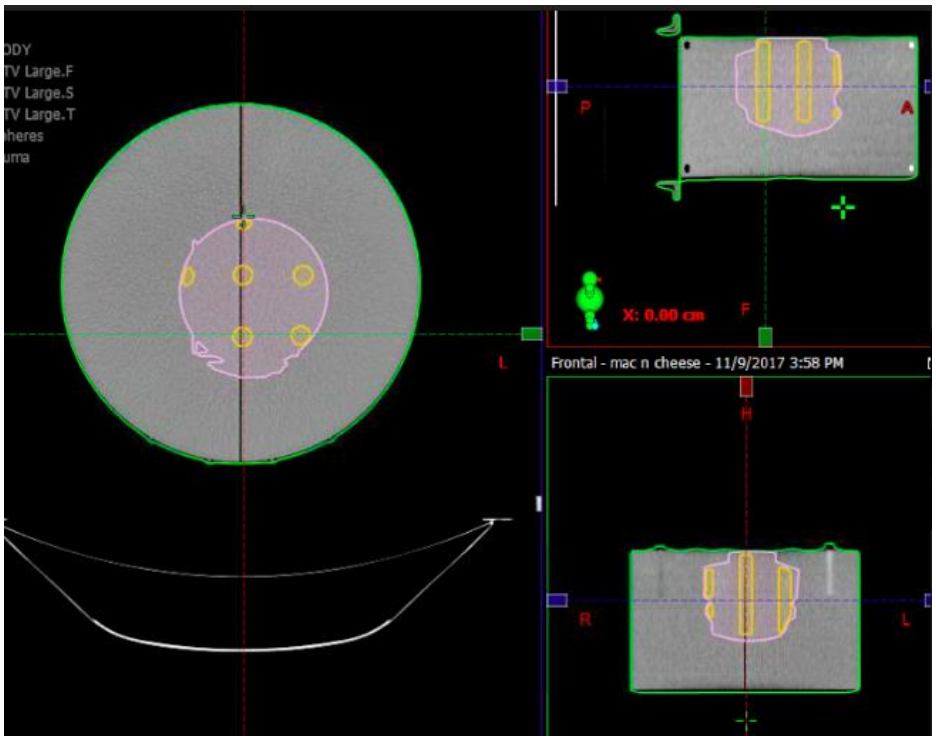

Figure 13. Superior Inferior GRID cores created with Eclipse TPS

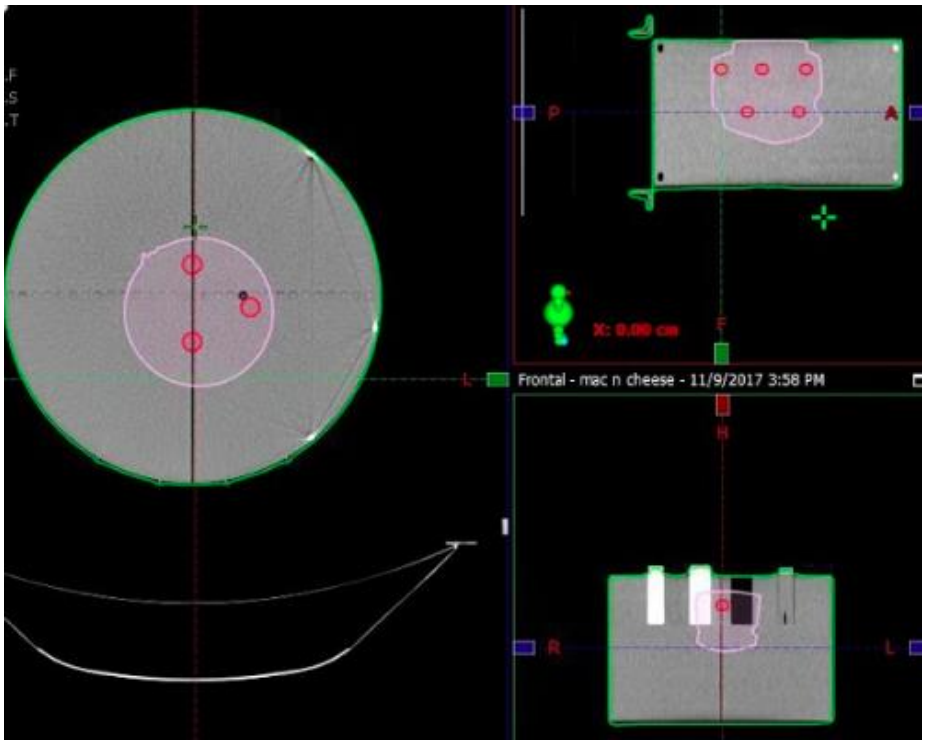

Figure 14. GRID spheres created with Eclipse TPS

The mock tumor GTV and GRID contours were then exported from our Eclipse TPS to the Tomotherapy HT-TPS for treatment planning and optimization. The plans were created with a pitch of 0.287, a fixed Jaw width of 1.05 cm, and a maximum modulation factor of 2. The treatment prescriptions mandated a 15 Gy to the treatments volume with 95% coverage. Once the plans had been optimized to a maximum achievable level, the plans were tested on the TomoHD unit and analyzed in the coronal plane with the PTW Octavius 729 ion chamber detector board and phantom, as well as the sagittal plane with EBT 3 Gafchromic film. Fractionated delivery was used to imitate the multiple passes expected in the real treatment scenario; fractions for each plan ranging from 10-14 mins were completed.

The PTW Mephysto GammaVision software was used in the comparison of the measured and calculated coronal dose planes for each plan. In following our clinical protocol after laser alignment of the phantom was achieved, a +2 mm adjustment was made in the z-axis to account for table sag. The film dosimetry was tested within the "cheese" phantom capturing the sagittal axis of the scan, and was analyzed using the red channel of an EPSON Expression 10000XL flatbed scanner and DoseLab comparison software.

Figure 15. Film Phantom Setup

The calibration films were exposed on a Varian Trilogy using the 6X - SRS energy at the dmax with a 100 cm source to surface distance (SSD). The calibration doses ranged from 0 to 450 cGy in 50 cGy increments. All films were scanned and calibrated at least 5 days after exposure to allow time for self-development and stabilization. Film data was used for high resolution relative dosimetry.

3. Results

3.1. Inferior/Superior Cores, 2D GRID Therapy

In optimizing the 2D GRID inferior/superior simulated cores, the maximum dose within the treatment cores was 24.24 Gy and the mean dose within the cores was 18.95 Gy. The minimum dose within the GTV, excluding the GRID region, was 1.35 Gy while the mean dose was 10.28 Gy. The phantom region outside of the treatment area received

a minimum dose of 0.02 Gy and a mean dose of 2.96 Gy. After optimization of the plan the total time to deliver to the plan was 73 minutes. Deliverable plans were achieved by fractionating the plan into 5 equal fractions of 14.6 minutes a piece.

The plan quality assurance was completed with the PTW ion chamber system. The results reported a gamma value of 95.6% at a distance-to-agreement of 2.0 mm and a dose difference with reference to the maximum dose of calculated volume of 2.0%. The film comparison was of measured fraction dose scaled to the full plan field dose cube. The measured film dose was normalized to a point of maximum dose by 5.886. The measured field was 1 of 5 fractions, meaning that the true measured fraction to plan fraction normalization value was only 1.17. With this film normalization the collected data showed a dose trough to peak percentage of roughly 45%.

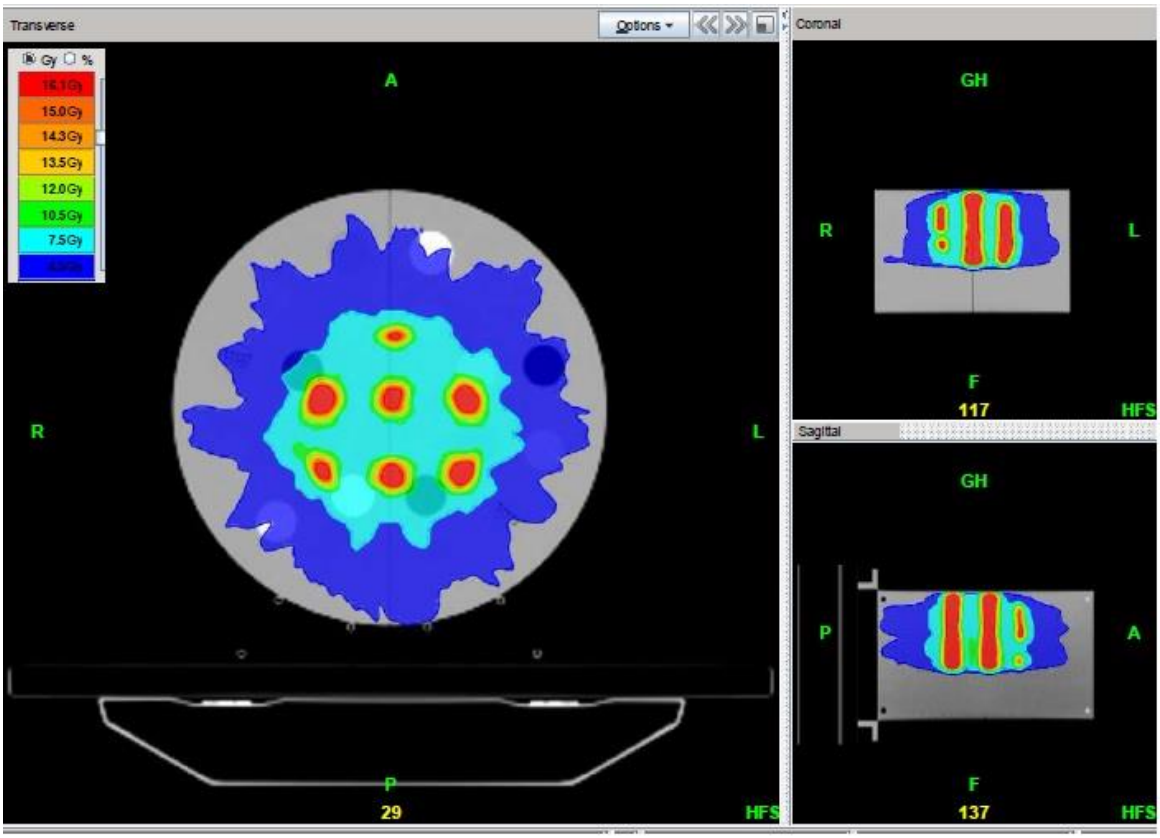

Figure 16. Planned Dose Distribution Inferior/Superior Cores

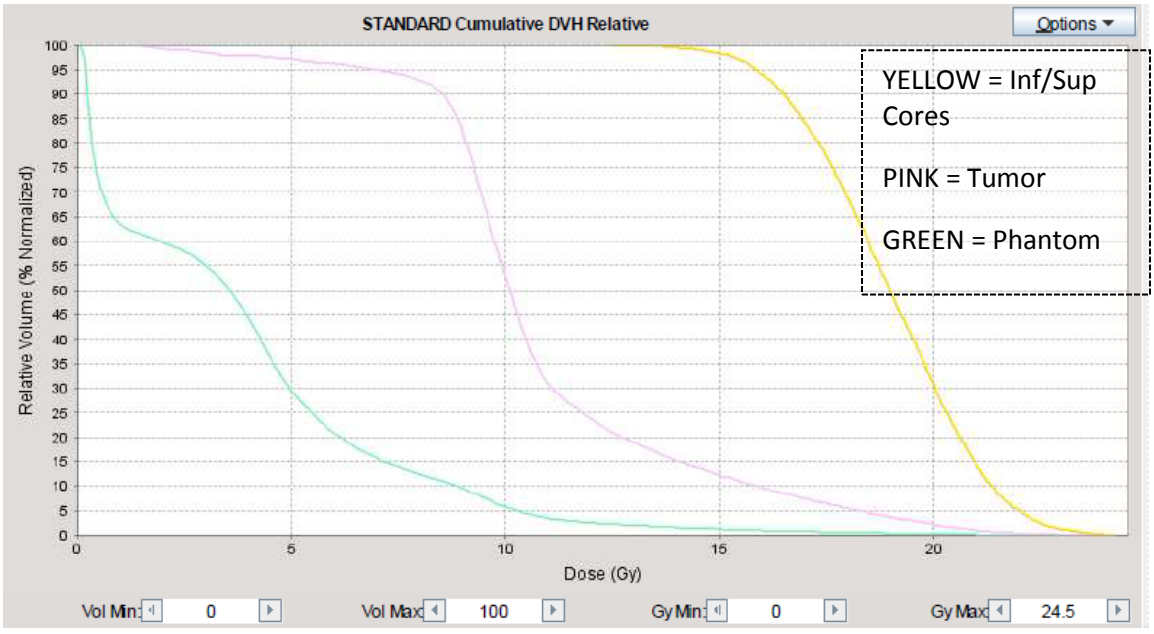

Figure 17. Dose Volume Histogram Inferior/Superior Cores

Total Plan Time: 73 min			**Fractionation Time:** (5 fx) 14.6 min		
Plan Dose: 15 Gy			**Fraction Dose:** 3 Gy		
Location	**Max Dose [Gy]**	**Min Dose [Gy]**	**Avg Dose [Gy]**	**StdDev Dose [Gy]**	**Physical Volume [cc]**
Inf/Sup Core	24.24	12.50	18.95	1.88	86.58
Phantom	19.23	0.07	2.96	3.57	12,943
Tumor	20.73	1.35	10.28	3.32	1,262

Table 1. Inferior/Superior Core Plan Data

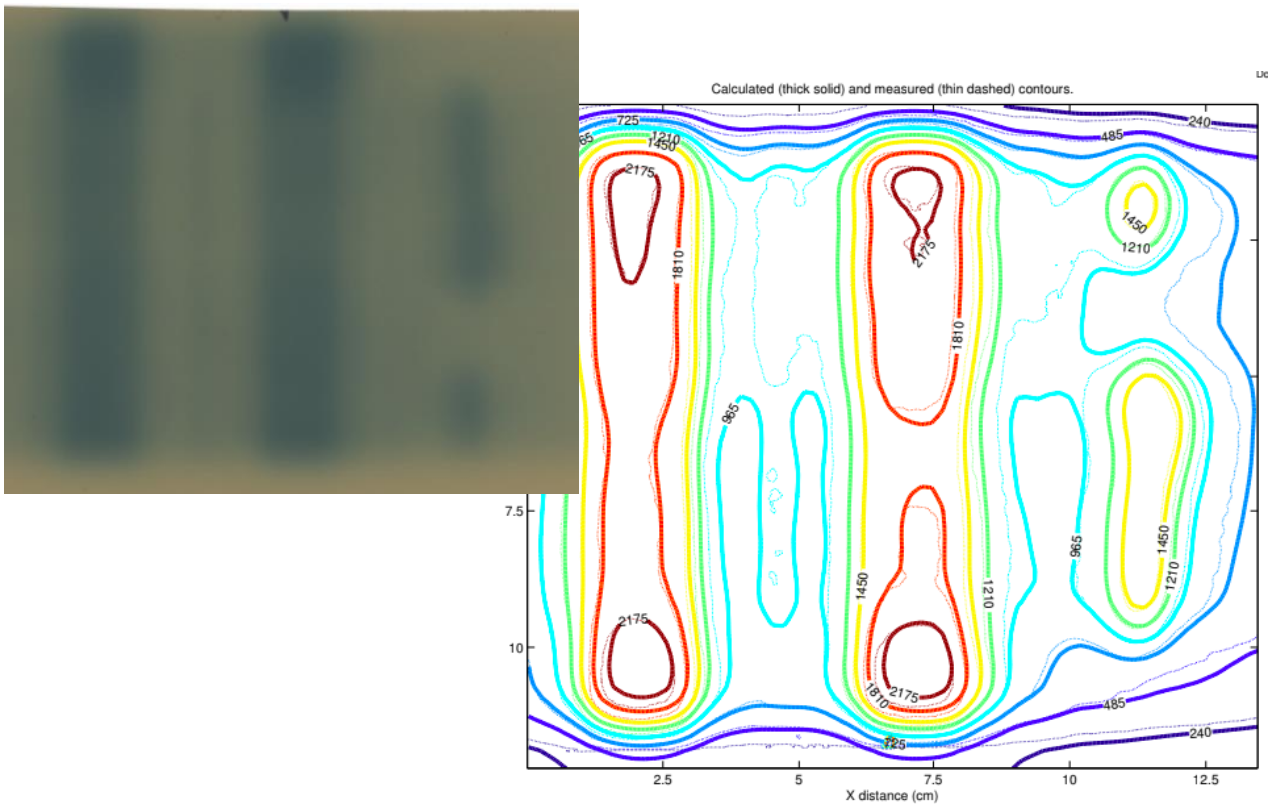

Figure 18. Scaled Single Fraction Sagittal Dose Plane Film Analysis, Inferior/Superior Cores

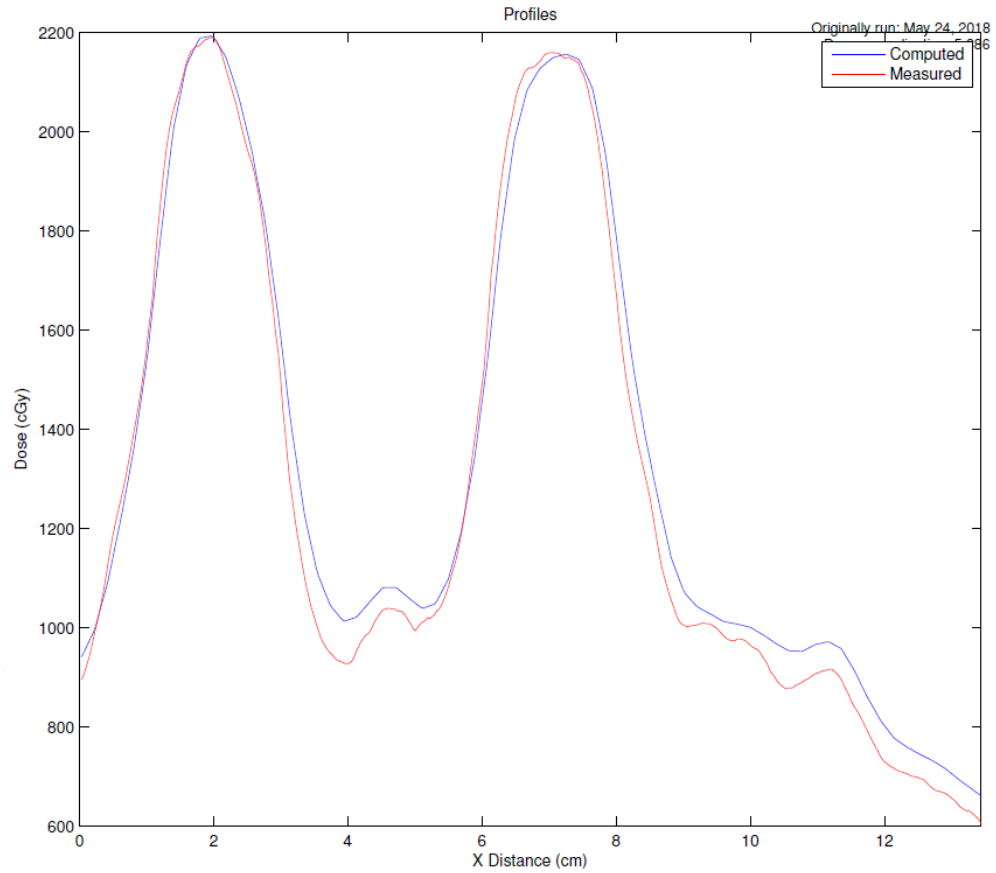

Figure 19. Dose Trough to Peak Film Data for Inferior/Superior Cores

3.2. Anterior/Posterior Cores, 2D GRID Therapy

In optimizing the 2D GRID anterior/posterior simulated cores, the maximum dose within the treatment cores was 24.24 Gy, and the mean dose within the cores was 18.07 Gy. The minimum dose within the GTV, excluding the GRID region, was 1.24 Gy while the mean dose was 6.84 Gy. The phantom region outside of the treatment area received a minimum dose of 0.05 Gy and a mean dose of 2.25 Gy. After optimization of the plan the total time to deliver to the plan was 96 minutes. Deliverable plans were achieved by fractionating the plan into 8 equal fractions of 12.0 minutes a piece.

The plan quality assurance was completed with the PTW ion chamber system. The results reported a gamma value of 99.2% at a distance-to-agreement of 2.0 mm and a dose difference with reference to the maximum dose of calculated volume of 2.0%. The film comparison was of measured fraction dose scaled to the full plan field dose cube. The measured film dose was normalized to a point of maximum dose by 9.594. The measured field was 1 of 8 fractions, meaning that the true measured fraction to plan fraction normalization value was only 1.20. With this film normalization the collected data showed a dose trough to peak percentage of roughly 12%.

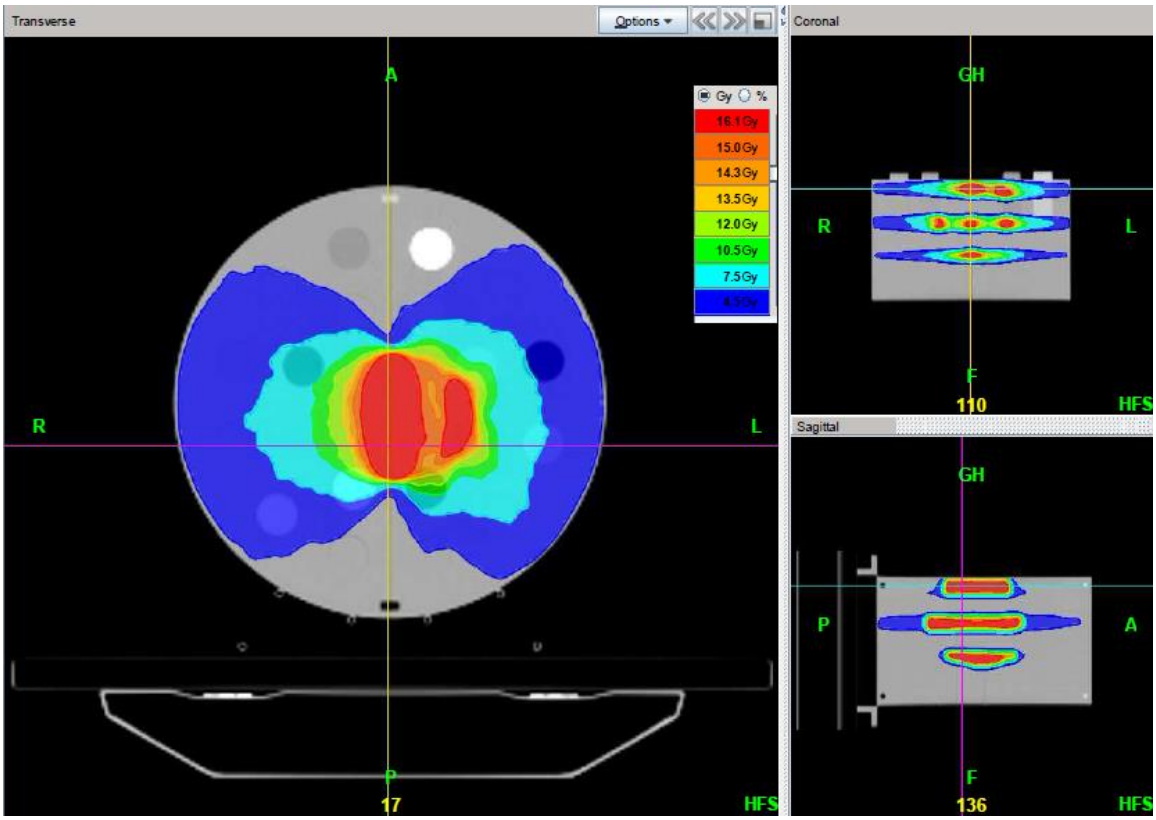

Figure 20. Planned Dose Distribution for Anterior/Posterior Cores

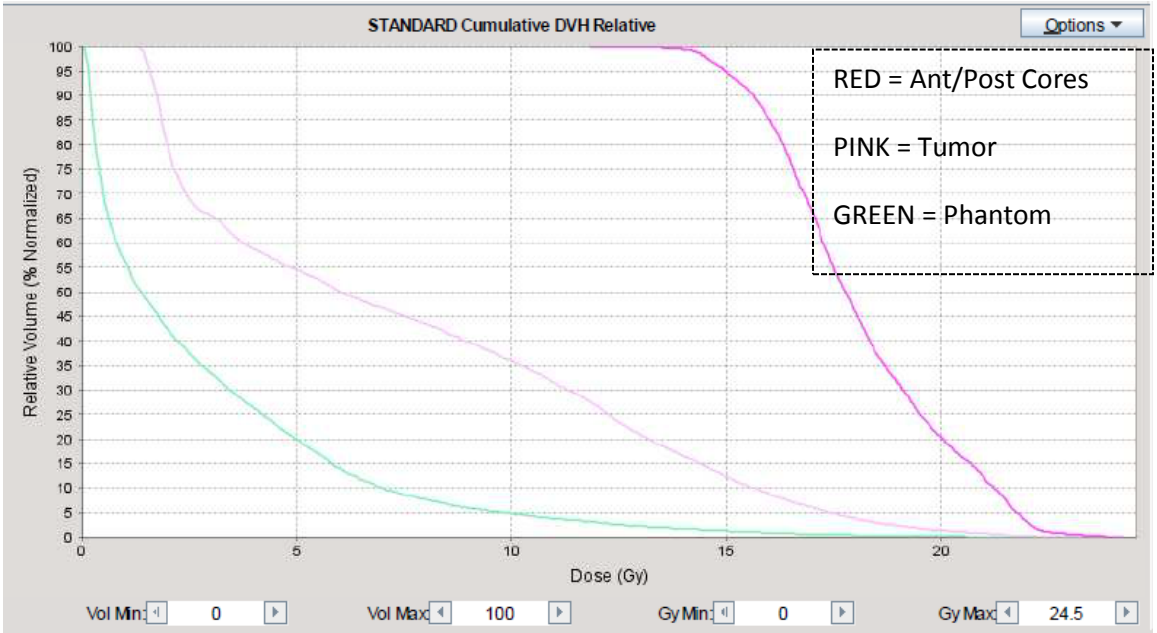

Figure 21. Dose Volume Histogram Anterior/Posterior Cores

Total Plan Time: 96 min			**Fractionation Time:** (8 fx) 12.0 min		
Plan Dose: 15 Gy			**Fraction Dose:** 1.87 Gy		
Location	**Max Dose [Gy]**	**Min Dose [Gy]**	**Avg Dose [Gy]**	**StdDev Dose [Gy]**	**Physical Volume [cc]**
Ant/Post Core	24.22	11.80	18.07	2.06	76.75
Phantom	19.14	0.05	2.25	3.37	12,943
Tumor	20.70	1.24	6.84	5.57	1,262

Table 2. Anterior/Posterior Core Plan Data

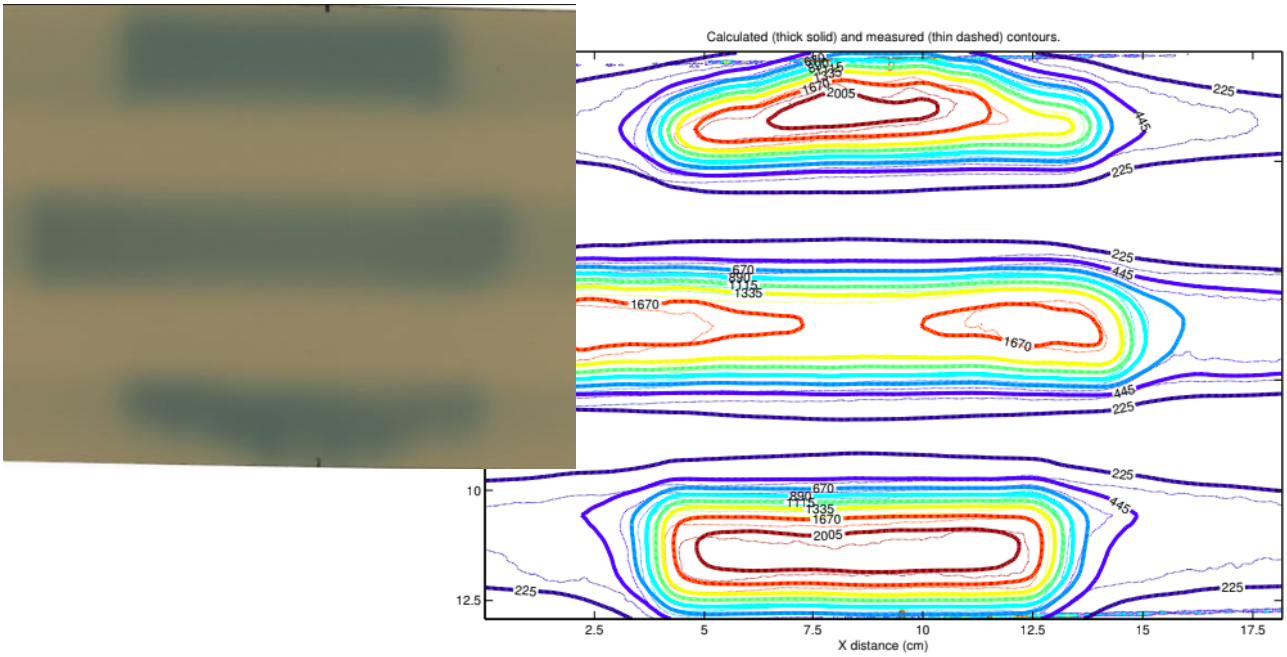

Figure 22. Scaled Single Fraction Sagittal Dose Plane Film Analysis, Anterior/Superior Cores

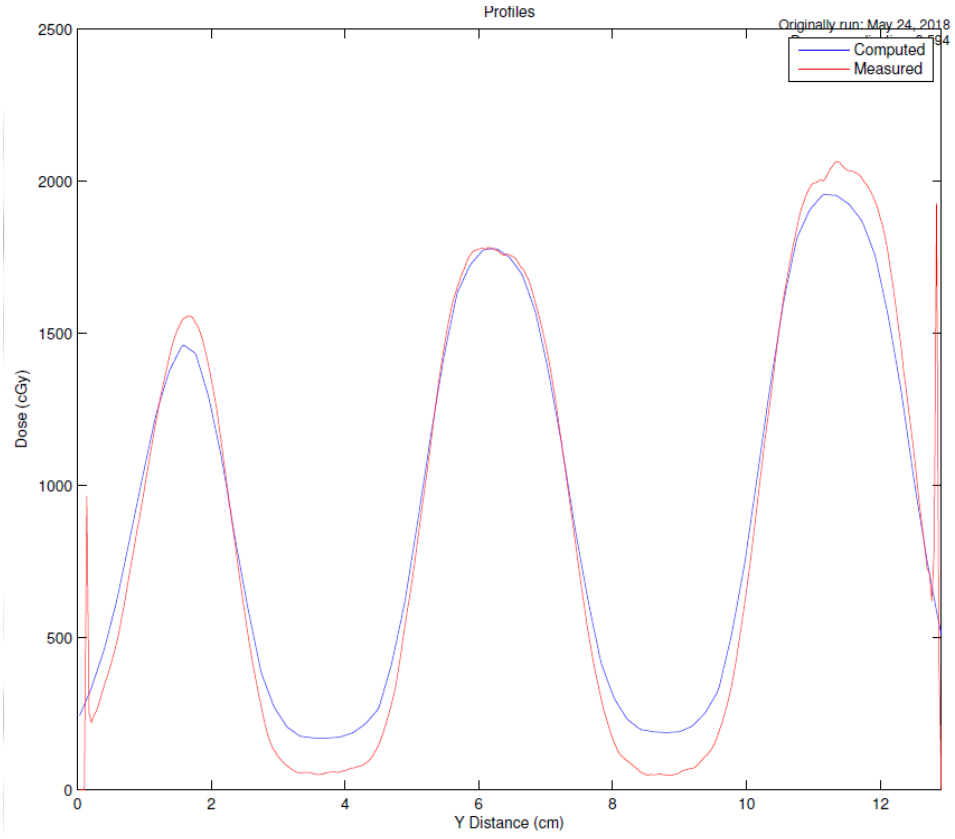

Figure 23. Dose Trough to Peak Film Data for Anterior/Posterior Cores

3.3. Spheres, 3D GRID Therapy

In optimizing the 3D GRID spheres, the maximum dose within the treatment spheres was 19.85 Gy, and the mean dose within the spheres was 16.94 Gy. The minimum dose within the GTV, excluding the GRID region, was 0.35 Gy while the mean dose was 3.46 Gy. The non-target phantom received a minimum dose of 0.02 Gy and a mean dose of 0.80 Gy. After optimization of the plan the total time to deliver to the plan was 44.4 minutes. Deliverable plans were achieved by fractionating the plan into 4 equal fractions of 11.1 minutes a piece.

The plan quality assurance completed with the PTW ion chamber system reported a gamma value of 100.0% at a distance-to-agreement of 2.0 mm and a dose difference with reference to the maximum dose of calculated volume of 2.0%. The film comparison was of measured fraction dose scaled to the full plan field dose cube. The measured film dose was normalized to a point of maximum dose by 4.688. The measured field was 1 of 4 fractions, meaning that the true measured fraction to plan fraction normalization value was only 1.17. With this film normalization the collected data showed a dose trough to peak percentage of roughly 32%.

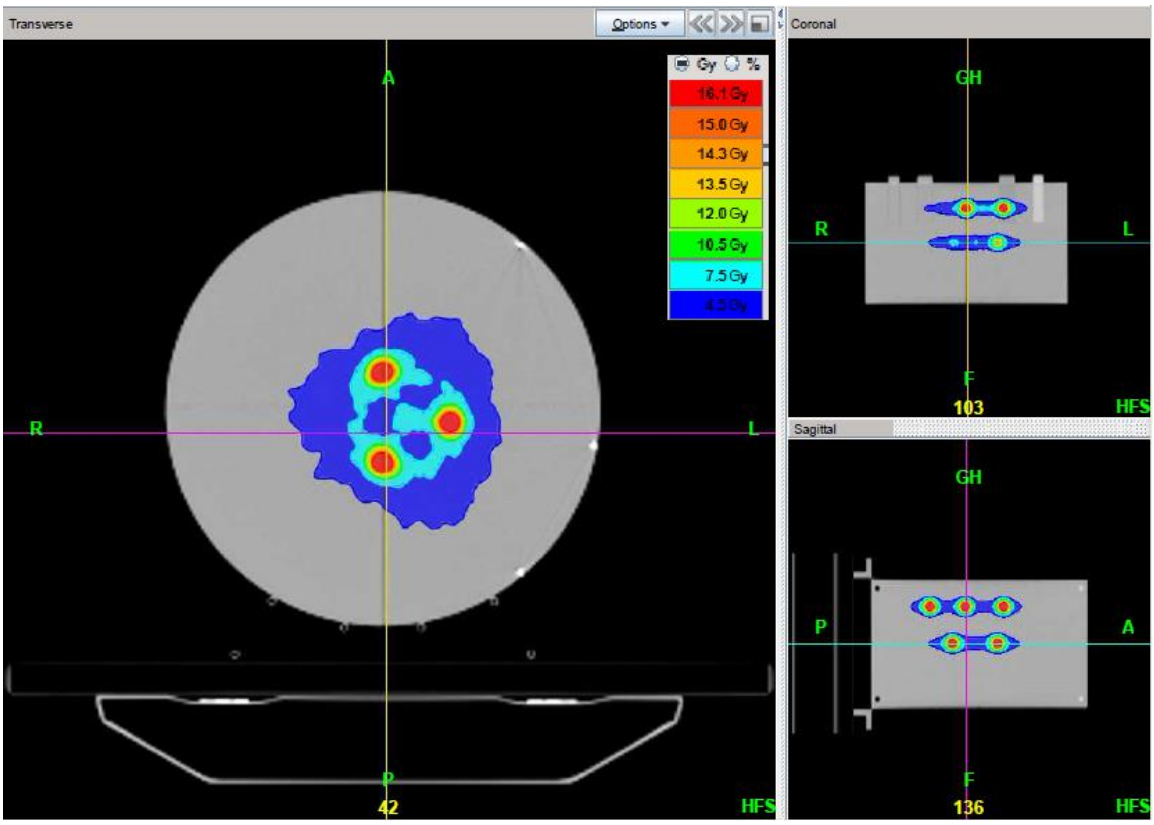

Figure 24. Planned Dose Distribution for Spheres

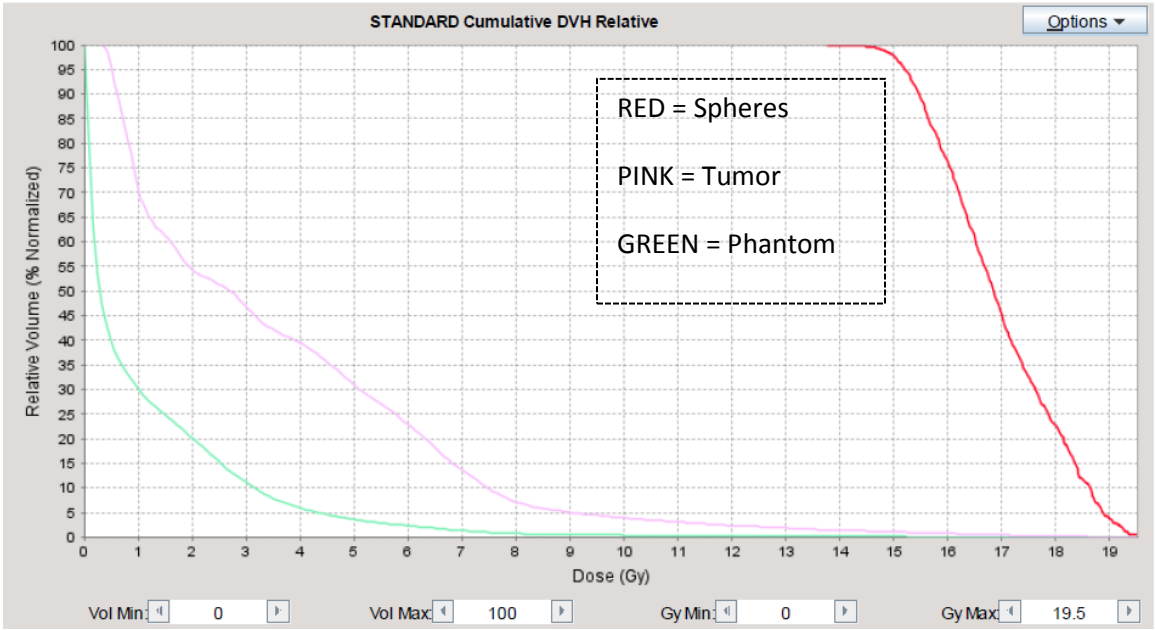

Figure 25. Dose Volume Histogram Spheres

Total Plan Time: 44.4 min			**Fractionation Time:** (4 fx) 11.1 min		
Plan Dose: 15 Gy			**Fraction Dose:** 3.75 Gy		
Location	**Max Dose [Gy]**	**Min Dose [Gy]**	**Avg Dose [Gy]**	**StdDev Dose [Gy]**	**Physical Volume [cc]**
Spheres	19.85	13.75	16.94	1.16	11.77
Phantom	9.83	0.02	0.80	1.69	12,943
Tumor	15.86	0.35	3.46	3.21	1,262

Table 3. Sphere Plan Data

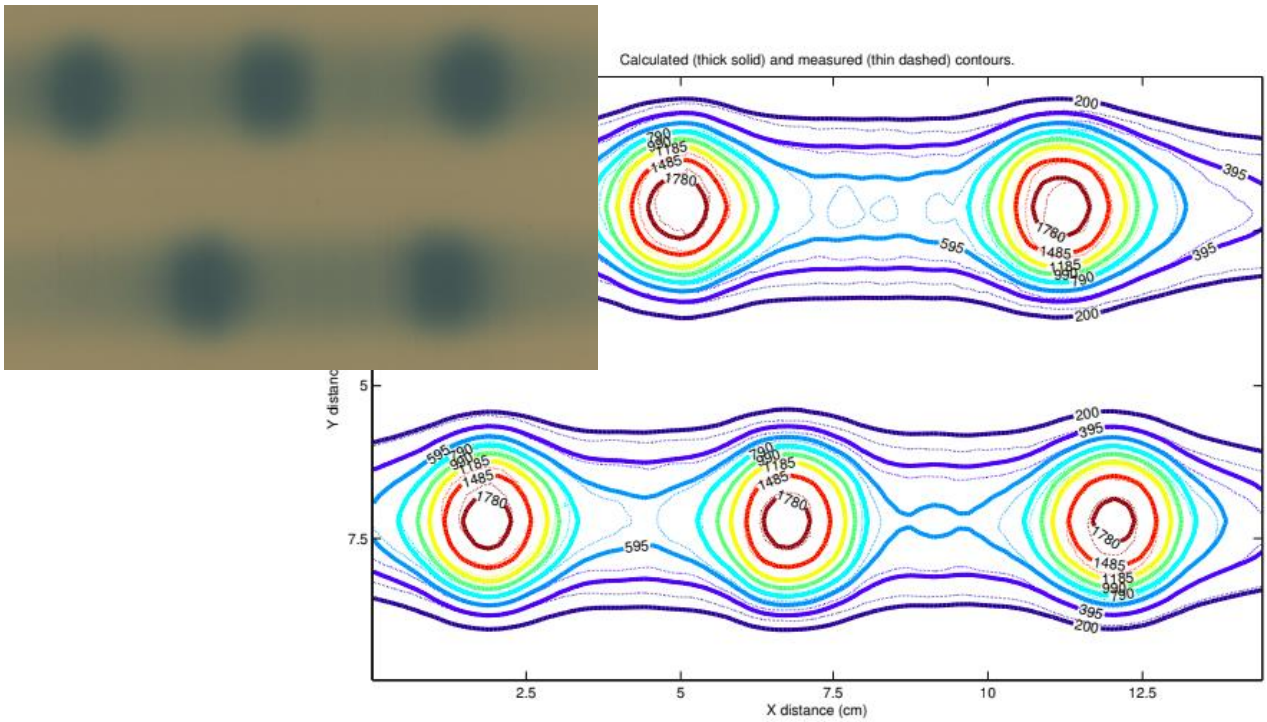

Figure 26. Scaled Single Fraction Sagittal Dose Plane Film Analysis, Spheres

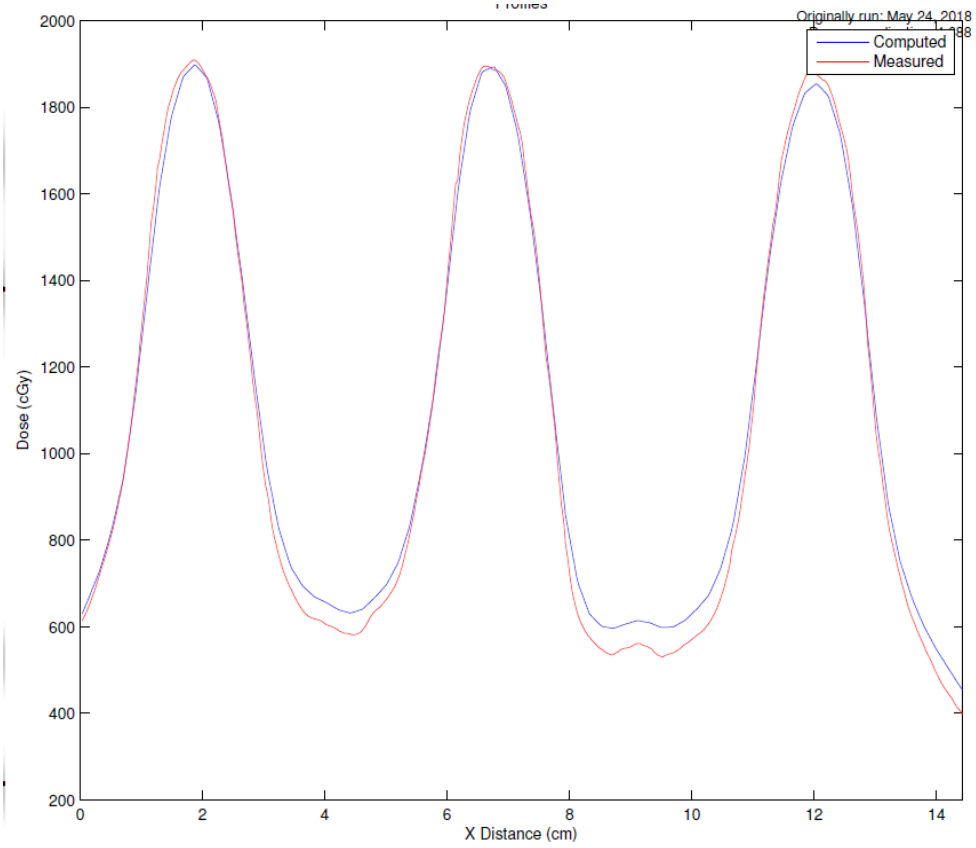

Figure 27. Dose Trough to Peak Film Data for GRID Spheres

4. Discussion

4.1. Clinical Feasibility

The paper published by UAMS reported acceptable dose distributions, clinical feasibility, and clinical results through the use of 2D GRID cores. These GRID cores had a diameter of 15 mm, a center to center geometry of roughly 40-50 mm, and a trough to peak percentage of roughly 50% [6], [7]. The 2D GRID cores investigated in this study showed similar dose distributions to those previously reported by UAMS, and even had better recorded trough to peak values. This was confirmed through fractionated

measurements of the plan. The times associated with the UAMS plans were not reported in the papers, so there is no way of comparing this parameter of the study.

However, the biggest question or concern with clinical feasibility in our clinic is the ability to run plans longer than roughly 15 minutes. Plans longer than 15 minutes often result in the machines water coolant system temperature to raise about 7° C, causing the machine to overheat and restart. Also the ability for patients to remain still on a treatment table for upwards of 40 minutes is approaching unreasonable, yet similar plans times have been achieved in our clinic. Asking a patient to remain still for over 40 minutes could be a struggle, and could result in delivery errors due to patient movement. With the control given by virtual GRID therapy a reasonable cropping of the dose around the GTV edges could be achieved, and would reduce the concern of patient movement.

There is the possibility of running the entire plan in fractions with 10 minute cool down times in-between fractions, but at 70 minutes this is not reasonable. This appears to be the biggest flaw in virtual GRID with the TomoTherapy treatment unit at this point. The planned dose distributions were acceptable, and all phantom contours appear to be receiving appropriate dose maximums. This was confirmed by plan quality assurance measurements.

4.2. 2D Core Comparison

In comparing the inferior/superior and anterior/posterior 2D GRID cores it appears that there are advantages and disadvantages to each method. The inferior/superior cores achieve a better dose reduction between all cores in the sagittal plane tested with film.

The dose reduction between the inferior/superior cores in the coronal plane where not as clear and defined. The inferior/superior plan was 73 minutes while the anterior/posterior plan was 96 minutes. The inferior/superior plan had higher mean and minimum doses in both the tumor volume and phantom volume. Also the inferior/superior plan achieved a higher average dose to the treatment cores.

In inspecting the dose volume histogram (DVH) for both 2D GRID cores, the anterior/posterior plan has decreased doses in its non-GRID volumes. Transferring this concept to a physical patient, the anterior/posterior plan would achieve better normal tissue sparing over all. The inf/sup plan appears to be better than the ant/post plan when looking at the 2D GRID core values. However the inferior/superior plan has one major flaw due to the lengthy times associated with achieving proper dose distributions.

4.3. 2D Versus 3D GRID

The papers previously published on lattices or 3D GRID therapy show a great promise with respect to clinical response and feasibility, yet only give limited information on the geometry of the sphere distribution. The only notes state that the spheres have a diameter of 15 mm [9], [10]. The spheres in the study match this one given parameter of 15 mm and are spaced our roughly 5 cm center-to-center. From a purely analytical standpoint, the 3D GRID spheres appear to be the better treatment option when compared to the 2D GRID cores. The sphere GRID therapy excels in almost every parameter measured in this study. The sphere plan has a lower treatment time of only 44.4 min and has lower minimum doses outside the treatment region. This plan has a

lower mean phantom dose, a lower minimum tumor dose, and a lower mean tumor dose. The only parameter in which the sphere plan fails is in the comparison of trough to peak measurement. This measurement is a simple test of dose conformity and drop off from the GRID treatment region and the non-GRID tumor.

Plan	Dose Trough/Peak Percentage
Inferior/Superior Core	(1000/2500) = 45.5%
Anterior/Superior Core	(250/2000) = 12.5%
Spheres	(600/1900) = 31.6%

Table 4. Dose - Trough to Peak Percentages

The most significant thing is the comparison of the DVH values for the 2D GRID plans with the 3D GRID sphere plan. With some inspection it is easy to see the significant reduction of the dose volumes within the normal phantom structure. This translates to an increased normal tissue sparing; a very important consideration for GRID therapy. This plan is still not a perfect candidate to clinically deliver in one pass. However, delivering this plan in 2 fractions of about 20 minutes paired with 10 minutes to cool off, this may be a realistic treatment method. There is also less clinical data and results supporting this methodology because it is a relatively new concept.

4.4. Future Directions

With the end goal of this research being to deliver GRID therapy to patients on the Helical TomoTherapy unit, more needs to be done before this treatment modality can be fully realized. With the plans in this study ranging from 45- 96 minutes, this is only feasible through multiple passes on the machine, resulting in a long scheduled treatment

time. Possible factors to investigate include: the GTV or mock tumor volume, treatment planning parameters, GRID geometry, and optimal GRID ratios.

A tumor volume of 1,250 cc is quite large and it is possible through the use of patient data, a more realistic tumor volume may be smaller and easier to treat. A study investigating the Helical TomoTherapy TPS pitch and jaw width settings showed that at every pitch value using a jaw size of 1 cm more than doubled the time to deliver similar plans with larger jaw settings[25]. Using this setting may greatly decrease treatment times by changing the jaw size in the treatment planning. This study did not investigate a variety of geometric distributions for the cores and spheres. It is possible that with a different geometries of spheres or cores, it may be easier for the machine these dose distribution, thus decreasing time for beam modulation. Finally, there is not an investigation on the optimal percentage of tumor volume receiving GRID Therapy. If an optimal yet minimal volume is found, this may allow for shorter treatment times.

Another topic to consider before clinical implementation is the difference in tissue densities or inhomogeneities in patients and phantoms. While these plans are technically feasible, the clinical aspects may change when you introduce all the new variables associated with an actual human patient. A collection of sample patients should be modeled and tested before any plans are ran on patients. In particular, patients with smaller transverse lesions associated with sarcomas may be of interest.

5. Conclusion

The results from this preliminary study indicate that it is possible to deliver high dose spatially fractionated plans with a Helical TomoTherapy unit. Both 2D cores and 3D spheres are possible. The data shows that with the current plan settings of pitch 0.287 and a fixed jaw setting of 1.05 cm the plans created have total delivery times that are greater than 40 minutes. These plans are too long for both the machine and patients to complete in one pass, so the plans needs to be fractionated to achieve deliverable times. The analysis of the 2D and 3D GRID plans indicate that the 3D GRID sphere geometry has the best qualities for treating real patients. The 3D GRID plan has the lowest treatment time and achieves planned dose maximums within the treatment cores, yet also has the lowest average non-target phantom dose. The quality assurance results show that the machine is completely capable of delivering the heterogeneous fields, but there is a complication requiring more scheduled time in order to reasonably achieve this in a clinical setting. This preliminary study indicates that with further investigation, the 3D GRID spheres show great promise for clinical implementation.

Table of Figures

Table of Tables

References

[1] G. Narayanasamy *et al.*, "Therapeutic benefits in grid irradiation on Tomotherapy for bulky, radiation-resistant tumors," *Acta Oncol.*, vol. 56, no. 8, pp. 1043–1047, Aug. 2017.

[2] W. V. Tenzel, "Experience with Grid Therapy," *Radiology*, vol. 59, no. 3, pp. 399–408, Sep. 1952.

[3] S. H. Benedict, "Review of Radiation Oncology Physics: A Handbook for Teachers and Students," *J. Appl. Clin. Med. Phys.*, vol. 5, no. 3, pp. 91–92, Jul. 2004.

[4] "Figure 1. Schematic diagram of human skin tissue model showing the...," *ResearchGate*. [Online]. Available: https://www.researchgate.net/figure/Schematic-diagram-of-human-skin-tissue-model-showing-the-thickness-d-melanin_fig1_261229613. [Accessed: 17-May-2018].

[5] G. A. Neuner, N. Vander Walde, J. K. Ha, C. X. Yu, M. Mohiuddin, and W. F. Regine, "High-dose Spatially-fractionated GRID Radiation Therapy (SFGRT): A Comparison of Outcomes of Treatment Delivered Through Cerrobend GRID versus MLC GRID," *Int. J. Radiat. Oncol.*, vol. 72, no. 1, Supplement, p. S488, Sep. 2008.

[6] X. Zhang *et al.*, "Application of Spatially Fractionated Radiation (GRID) to Helical Tomotherapy using a Novel TOMOGRID Template," *Technol. Cancer Res. Treat.*, vol. 15, no. 1, pp. 91–100, Feb. 2016.

[7] Zhang Xin *et al.*, "Spatially fractionated radiotherapy (GRID) using helical tomotherapy," *J. Appl. Clin. Med. Phys.*, vol. 17, no. 1, pp. 396–407, Jan. 2016.

[8] W. X, A. M. M, W. J, G. S, and P. A, "On Modern Technical Approaches of Three-Dimensional High-Dose Lattice Radiotherapy (LRT)," *Cureus*, vol. 2, no. 3, Mar. 2010.

[9] B. E. Amendola *et al.*, "LATTICE Radiotherapy with RapidArc for Treatment of Gynecological Tumors:Dosimetric and Early Clinical Evaluations," *Cureus*, Sep. 2010.

[10] B. E. Amendola, N. C. Perez, X. Wu, J. M. Blanco Suarez, J. J. Lu, and M. Amendola, "Improved outcome of treating locally advanced lung cancer with the use of Lattice Radiotherapy (LRT): A case report," *Clin. Transl. Radiat. Oncol.*, vol. 9, pp. 68–71, Jan. 2018.

[11] S. Gholami, H. A. Nedaie, F. Longo, M. R. Ay, S. Wright, and A. S. Meigooni, "Is grid therapy useful for all tumors and every grid block design?," *J. Appl. Clin. Med. Phys.*, vol. 17, no. 2, pp. 206–219, Mar. 2016.

[12] M. Mohiuddin, H. Park, S. Hallmeyer, and J. Richards, "High-Dose Radiation as a Dramatic, Immunological Primer in Locally Advanced Melanoma," *Cureus*, vol. 7, no. 12.

[13] A. Kaiser, M. M. Mohiuddin, and G. L. Jackson, "Dramatic response from neoadjuvant, spatially fractionated GRID radiotherapy (SFGRT) for large, high-grade extremity sarcoma," *J. Radiat. Oncol.*, vol. 2, no. 1, pp. 103–106, Mar. 2013.

[14] "History of Radiation: Brief History of Ionizing Radiation & Radioactivity," *Mirion*. [Online]. Available: https://www.mirion.com/introduction-to-radiation-safety/the-history-of-radiation/. [Accessed: 23-May-2018].

[15] S. Gianfaldoni, R. Gianfaldoni, U. Wollina, J. Lotti, G. Tchernev, and T. Lotti, "An Overview on Radiotherapy: From Its History to Its Current Applications in

Dermatology," *Open Access Maced. J. Med. Sci.*, vol. 5, no. 4, pp. 521–525, Jul. 2017.
[16] E. J. Hall and A. J. Giaccia, *Radiobiology for the radiologist*, 7th ed. Philadelphia: Wolters Kluwer Health/Lippincott Williams & Wilkins, 2012.
[17] R. Asur, K. T. Butterworth, J. A. Penagaricano, K. M. Prise, and R. J. Griffin, "High dose bystander effects in spatially fractionated radiation therapy," *Cancer Lett.*, vol. 356, no. 1, pp. 52–57, Jan. 2015.
[18] M. Najafi, R. Fardid, G. Hadadi, and M. Fardid, "The Mechanisms of Radiation-Induced Bystander Effect," *J. Biomed. Phys. Eng.*, vol. 4, no. 4, pp. 163–172, Dec. 2014.
[19] "The Impact of TNF-α Induction on Therapeutic Efficacy following High Dose Spatially Fractionated (GRID) Radiation," vol. 1, no. 2, p. 7, 2002.
[20] S. B. Jakowlew, "Transforming growth factor-beta in cancer and metastasis," *Cancer Metastasis Rev.*, vol. 25, no. 3, pp. 435–457, Sep. 2006.
[21] R. S. Asur *et al.*, "Spatially Fractionated Radiation Induces Cytotoxicity and Changes in Gene Expression in Bystander and Radiation Adjacent Murine Carcinoma Cells," *Radiat. Res.*, vol. 177, no. 6, pp. 751–765, Jun. 2012.
[22] "TomoTherapy System," *Precise, Innovative Tumor Treatments | Accuray*. .
[23] "Schematic drawing of a helical tomotherapy unit.," *ResearchGate*. [Online]. Available: https://www.researchgate.net/figure/Schematic-drawing-of-a-helical-tomotherapy-unit_fig2_51166856. [Accessed: 31-May-2018].
[24] H. Geng, C. Kong, W. Lam, K. Cheung, and S. Yu, "The Impact of Thread Effect on Tomotherapy Quality Assurance With 4D Detector Array," *Int. J. Radiat. Oncol. • Biol. • Phys.*, vol. 87, no. 2, pp. S576–S577, Oct. 2013.
[25] M. Moldovan *et al.*, "Investigation of Pitch and Jaw Width to Decrease Delivery Time of Helical Tomotherapy Treatments for Head and Neck Cancer," *Med. Dosim.*, vol. 36, no. 4, pp. 397–403, Dec. 2011.